Automatic segmentation of a cerebral glioblastoma using a smart computational technique

Segmentación automática de glioblastoma cerebral usando una técnica computacional inteligente

Miguel Vera MSc, PhD[1,2]*, https://orcid.org/0000-0001-7167-6356, Yoleidy Huérfano MSc[2], https://orcid.org/0000-0003-0415-6654, Oscar Valbuena MSc[3] https://orcid.org/0000-0003-3080-8839, Diego Hoyos[4] , Yeni Arias[4], Yudith Contreras MSc[1] https://orcid.org/0000-0003-4358-730X, Williams Salazar MD[5] https://orcid.org/0000-0001-5669-6105,, María Isabel Vera BSc[5] https://orcid.org/0000-0003-1135-6283,, Maryury Borrero MSc[1], https://orcid.org/0000-0003-3025-1321, Marisela Vivas, MSc, PhD[6] https://orcid.org/0000-0002-8941-4562, https://orcid.org/0000-0002-8941-4562, Carlos Hernández MSc[1] https://orcid.org/0000-0001-8906-1982, https://orcid.org/0000-0001-8906-1982, Doris Barrera MSc[1], https://orcid.org/0000-0002-6443-6757, Ángel Valentín Molina MSc[7], https://orcid.org/0000-0001-9604-7222, Luis Javier Martínez PhD[7], https://orcid.org/0000-0003-0917-9847, Juan Salazar MSc[1], https://orcid.org/0000-0001-6826-203X, Elkin Gelvez MSc[1], https://orcid.org/0000-0001-5157-3341, Frank Sáenz MSc[4], https://orcid.org/0000-0001-9604-7220.

[1]Universidad Simón Bolívar, Facultad de Ciencias Básicas y Biomédicas, Cúcuta, Colombia. *E-mail de correspondencia: m.avera@unisimonbolivar.edu.co
[2]Grupo de Investigación en Procesamiento Computacional de Datos (GIPCD-ULA), Universidad de Los Andes-Táchira, Venezuela.
[3]Grupo de Investigación en Educación Matemática, Matemática y Estadística (EDUMATEST), Facultad de Ciencias Básicas, Universidad de Pamplona.
[4]Universidad Simón Bolívar, Facultad de Ingeniería, Cúcuta, Colombia.
[5]Servicio de Neurología, Hospital Central de San Cristóbal-Táchira, Venezuela.
[6]Universidad Simón Bolívar, Departamento de Ciencias Sociales y Humanas, Cúcuta, Colombia.
[7]Grupo de Investigación en Ingeniería Clínica - HUS (GINIC-HUS), Vicerrectoría de Investigación, Universidad ECCI.

Abstract

We propose an intelligent computational technique for the image segmentation of a type IV brain tumor, identified as multiform glioblastoma (MGB), which is present in multi-layer computed tomography images. This technique consists of 3 stages developed in the three-dimensional domain. They are: pre-processing, segmentation and validation. During the validation stage, the Dice coefficient (Dc) is considered in order to compare the segmentations of the MGB, obtained automatically, with the segmentations of the MGB generated manually, by a neuro-oncologist. The combination of parameters linked to the highest Dc, allows to establish the optimal parameters of each of the computational algorithms that make up the proposed nonlinear technique. The obtained results allow to report a Dc higher than 0.88, validating a good correlation between the manual segmentations and those produced by the computational technique developed.

Keywords: Brain Tomography, Cerebral Tumor, Glioblastoma, Intelligent Computational Technique, Segmentation.

Resumen

Proponemos una técnica computacional inteligente para la segmentación de imágenes de un tumor cerebral tipo IV, identificado como glioblastoma multiforme (MGB), que está presente en imágenes de tomografía computarizada de múltiples capas. Esta técnica consiste en 3 etapas desarrolladas en el dominio tridimensional. Ellos son: preprocesamiento, segmentación y validación. Durante la etapa de validación, se considera el coeficiente de dados (Dc) para comparar las segmentaciones del MGB, obtenidas automáticamente, con las segmentaciones del MGB generado manualmente, por un neurooncólogo. La combinación de parámetros vinculados a la mayor Dc permite establecer los parámetros óptimos de cada uno de los algoritmos computacionales que conforman la técnica no lineal propuesta. Los resultados obtenidos permiten informar una Dc superior a 0,88, validando una buena correlación entre las segmentaciones manuales y las producidas por la técnica computacional desarrollada.

Palabras clave: Tomografía cerebral, Tumor cerebral, Glioblastoma, Técnica computacional inteligente, Segmentación.

Introduction

The segmentation of anatomical structures of the human brain, present in images acquired by any imaging modality, constitutes the starting point for the diagnosis of a high number of diseases or pathologies that affect the brain. Among these pathologies are brain tumors which originate from several cell lines and are classified according to various criteria[1]. One of them is according to the place of the body where they are generated. In this sense, they can be classified into two groups:

a) Primary tumors. Space-occupying lesions (SOL) that start in the brain and tend to remain there. b) Secondary tumors.

SOL that originate in other sites of the human body and spread and/or infiltrate the brain[2,3], as metastasis. The most frequent primary tumors are glioblastomas and meningiomas; while the most frequent metastases come from cancers in skin, lungs and breast[1,2,3].

The World Health Organization (WHO)[4] uses the degree of malignancy of the tumor as a criterion to classify primary tumors into four grades. According to this classification, tumors labeled with grades I and II are generally benign; while those classified in grades III and IV are considered malignant. Normally, patients with primary grade I brain tumors have a longer survival than those with grade IV tumors[1,2].

For the present study, the tumors reported in the literature, such as multiforme glioblastomas, are of special interest. According to WHO[4], multiforme glioblastomas can be located in the context illustrated in figure 1.

Figure 1. Block diagram in which the brain tumor, considered in the present work, has been greyed out and it is identified as multiform gliobastoma.
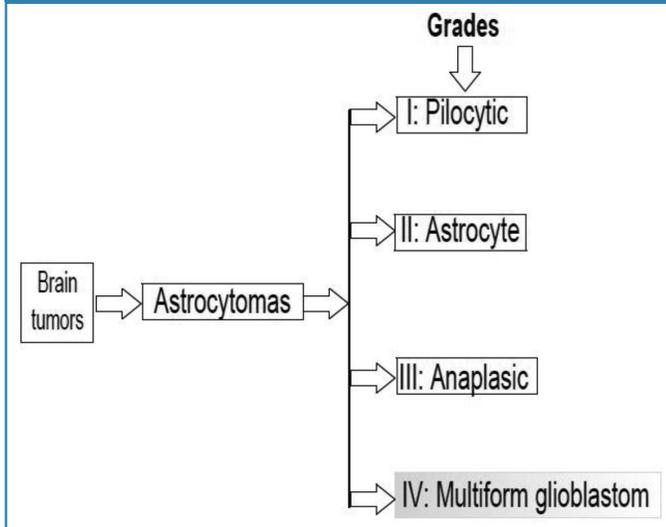
As indicated in figure 1, tumors of the astrocytoma type are found among brain tumors, and multiform glioblastomas (MGB) appear within that group. Normally, tumors of the MGB type, have central necrotic areas due to their rapid growth within the surrounding normal brain tissue, the cells look crowded strange at the microscope[3]. These tumors form new blood vessels to maintain their rapid growth[5]. In addition, they are diagnosed in 45-60% of cases, with a predominant incidence in males between 45 and 65 years. This type of tumor represents 20% of intracranial tumors, 55% of gliomas and 80% of gliomas in the cerebral hemispheres of adults and is the tumor with the worst survival rate at one year (39.3%) and at 3 years (5.5%)[5]. In addition, every year more than 66,000 inhabitants of the USA, are diagnosed with a primary brain tumor and more than twice that amount are diagnosed with a metastatic brain tumor[4,5].

Regarding neuroimages, cerebral digital ones are accompanied by various imperfections such as noise[6,7] and artifacts[8] which affect the quality of information associated with the anatomical structures that make up these images. These imperfections become real challenges, when computational strategies are implemented to generate the morphology (normal or abnormal) of the mentioned structures[6]. By way of example, figure 2, generated on the basis of multi-layer computed tomography (MSCT), illustrates the presence of Poisson noise, the stair artifact and the low contrast between brain structures.

Figure 2. Axial views of brain CT images in which one can observe: a) Poisson noise. b) Artifact (see red arrow). c) Low contrast between lobular structures.
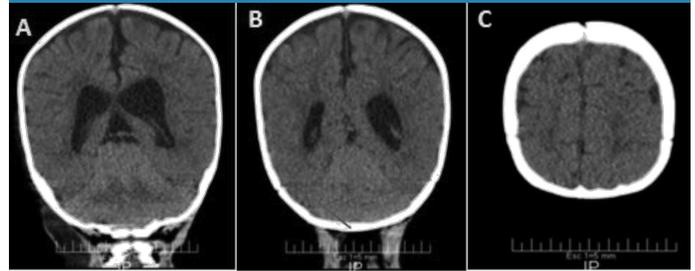
Reviewing the state of the art regarding tumor segmentation, the works described below were found: Casamitjana et al.[9] constructed 3D convolutional neural networks to classify tumors and tumor subsections in brain MRI images. The best three-dimensional neural network reached a Dice (Dc) coefficient of 0.9174.

Similarly, Zhang et al.[10], proposed a totally convolutional neural network (FCNN), where several classical FCNN architectures are applied to the 2D sections of the brain magnetic resonance imaging. They evaluated the performance of the network using the Dc whose average value was 0.9050.

Kleesiek et al.[11], present the ilastik application as a tool for the segmentation of brain tumors in multimodal magnetic resonance imaging. They used the images contained in the Brain Tumor Segmentation Challenge-2013 database. Their proposed technique uses the normalization of the data using, as a reference, the mean value of the cerebrospinal fluid. On these normalized data they applied a segmentation process based on the predictions of the probabilistic algorithm called random forest. Finally, the automatic segmentations are compared with the manual ones using the Dc whose average value was 0.79.

On the other hand, the present work proposes a smart computational technique (SCT) for the segmentation of an MGB type tumor, present in a database formed by three-dimensional brain images of MSCT. This technique comprises the stages of pre-processing, segmentation and validation using the Dice coefficient[6] so as to compare segmentations of the MGB, obtained automatically and manually.

Materials and methods

Description of the databases
The database (DB) used was provided by the Central Hospital of San Cristóbal-Táchira-Venezuela. It was acquired through the MSCT modality and consists of three-dimensional images (3D), corresponding to the anatomical structures present in the head of 1 a male patient. Numerical characteristics are presented on table 1.

| Table 1. General characteristics of the database considered in the present work.					
DB	Voxels	Voxels dimensions	Scanner type		Age
Label	number	(mm³)			(years)
DB1	512x512x24	0.2773 x 0. 2773 x	*GE Light Speed VCT		50
		2.1744	IRIS		

*GE= General Electric.

As a complement, for comparison, manual segmentation is available, generated by a neuro-oncologist, corresponding to the MGB present in the DB considered. This segmentation represents the ground truth that will serve as a reference to validate the results.

Description of the proposed computational technique, for the automatic segmentation of the MGB.

Figure 3 is a schematic diagram synthesizing the methods that make up the proposed technique to segment the tumor.

Figure 3. Block diagram of the SCT proposed for the segmentation of the MGB tumor.
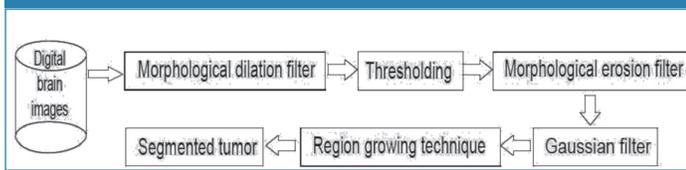
Pre-processing Stage
In the block diagram (Figure 3), this stage corresponds to the techniques: dilation, thresholding, morphological erosion and Gauss smoothing. Each of them is described forthwith.

o   Morphological Dilation Filter (MDF):

Since mathematical morphology is based on set theory, the objects present in an image can be treated as sets of points[12]. Generally, it is possible to define operations between two sets, one consisting of elements belonging to the aforementioned objects and another set called structuring element (SE)[13]. SEs can be visualized as neighborhoods of the element under study, which have variable morphology. [14].

In practice, mathematical morphology is implemented through various morphological filters whose basic operators are dilation and erosion[13,14]. These operators are non-linear spatial filters that can be applied to binary, grayscale or color images. In particular, the dilation (⊕) of a two-dimensional image (I), composed of gray levels, using a two-dimensional SE, is defined by Equation 1[15].

$$(I \oplus SE)(x,y) = \max_{(s,t)\,\epsilon\,B}[I(x+s,y+t) - SE(s,t)]. \quad (1)$$

Where: *max* is the maximum gray level contained in *SE*, *(s, t)* defines the size of the *SE* and *(x, y)* represents the position of the pixel under study.

According to equation 1, to apply the filter or morphological dilation operator the image considered with an SE or neighborhood, of arbitrary size, is covered, replacing the gray level of each of the elements of such an image by the level ofgray maximum, contained in the aforementioned neighborhood. For the purposes of this work, a cubic structuring element was considered and the size of said SE is left as a parameter to control the performance of the MDF.

o   Thresholding:

The thresholding algorithms are, generally, simple structures and allow to classify, efficiently, the elements of an image considering one or several thresholds. Such thresholds can be selected by considering both the histogram of an image and the position, intensity or an arbitrary neighborhood of the element under study, often called the current element[16]. In the present work a simple threshold was considered, which is based on the choice of a value for a certain threshold. This threshold allows discrimination between the anatomical structure of interest and the rest of the structures present in an image. Usually, the referred threshold is chosen considering the histogram of the image. One of the criteria applied to perform the aforementioned discrimination is the following: *If the intensity or gray level of the current element is equal to or less than the selected threshold value, the gray level (GL) of the current element remains unchanged; while if such intensity is greater than GL of the current element, it is generally correlated with the lower level of gray present in the image being processed*[16].

o   Morphological Erosion Filter (MEF):

The erosion (Θ) of a two-dimensional image (I), composed of gray levels, using a two-dimensional SE, is defined by Equation 2[14,15].

$$(I \ominus SE)(x,y) = \min_{(s,t)\,\epsilon\,B}[I(x+s,y+t) - SE(s,t)] \quad (2)$$

Where: *min* the minimum gray level contained in *SE*, *(s, t)* defines the size of the *SE* and *(x, y)* represents the position of the pixel under study.

According to equation 2, to apply the filter or morphological erosion operator the image considered with an SE or neighborhood, of arbitrary size, is covered, replacing the gray level of each of the elements of such image by the level of gray minimum, contained in the aforementioned neighborhood. For purposes of the present work, a cubic structuring element was considered and the size of said SE is left as a parameter to control the performance of the MEF.

o Gaussian Filtering (GF):

The purpose of the Gaussian filter is to address the problem of noise. The Gaussian filter is characterized as a linear spatial technique that has been used classically to minimize the noise present in images. There is a relationship between the

amount of noise that is attenuated by the application of this filter and the blurring of the image[17]. This type of filter uses a discrete Gaussian distribution which can be expressed by means of a Gaussian mask or kernel, of arbitrary size. For example, in order to soften, a 3-D image, the scalars that make up the aforementioned kernel can be obtained according to equation 3.

$$G(i, j, k) = \frac{1}{\left(\sqrt{2\pi}\right)^3 \sigma_i \sigma_j \sigma_k} e^{-\left(\frac{i^2}{2\sigma_i^2} + \frac{j^2}{2\sigma_j^2} + \frac{k^2}{2\sigma_k^2}\right)} \quad (3)$$

Where: $0 \leq i, j, k \leq (n - 1)$, n is the size of the Gaussian kernel, σ_i, σ_j and σ_k the standard deviations for each spatial dimension. In practice, in the present work, Gaussian filtering is implemented by convolving the Igs image with the aforementioned Gaussian kernel[17]. The parameters of this filter are: the standard deviation of each of the spatial dimensions and the radius (r) that defines the size (n) of the mask, given by equation 4.

$$n = 2r + 1, \quad (4)$$

Where r is an arbitrary scalar value. It is important to note that, in the present work, an isotopic approach is assumed whereby the standard deviation, of each spatial dimension, of the Gauss filter is matched with the standard deviation of the image processed by morphological erosion.

Segmentation Stage

● Computer intelligence operators: Support Vector Machines (SVM).

Support vector machines (SVM) are paradigms that undergo training and detection processes, and are based on both the Vapnik-Chervonenkis learning theory and the minimization principle that considers structural risk[18]. SVM can be considered as classification and functional approach tools[19,20]. A variant of the SVM, called the least squares vector support machine (LSSVM), can be obtained using robust statistics, Fisher discriminant analysis and replacing the system of in-equations that govern the SVM, by an equivalent system of linear equations, which can be solved more efficiently[21,22]. Additionally, unlike other learning-based classification systems such as artificial neural networks (NN), LSSVMs use the criterion of minimization of structural risk, which raises the generalization capacity of the aforementioned machines to optimum levels, making it possible for LSSVM perform adequately in the validation process, surpassing NN in this aspect, which uses empirical risk[23].

In this work, the location of the seed voxel, to initialize the segmentation technique called region growth (RG)[13], is calculated using LSSVM. There are several functions that can be considered to construct the decision surface that allow the vector support machines to identify the seed. For purposes of the present work, a Gaussian radial base function (RBF) is considered and, therefore, a formulation is obtained that depends on the hyperparameters, identified as: a) Error penaltyparameter (γ) and b) Parameter to control the selectivity (σ^2) of the LSSVM.

In this sense, the LSSVMs call for a process of intonation of such hyperparameters. Theoretically, both parameters can assume values that belong in the range of real numbers comprised between 0 and infinity[21,22]. The intonation process is necessary because it is very difficult to know, a priori, the combination of values that will generate optimal results when the LSSVM carry out the training and validation processes.

Additionally, to identify automatically the coordinates of the seed voxel, the following procedure was implemented:

i) A size reduction technique, based on bicubic interpolation, optimal reduction factor, is applied to match the one obtained in[6]. This allows to generate sub-sampled images of 64x64 pixels from filtered images of 512x512, that is, the mentioned factor is 8.

ii) A neurosurgeon selects, on the sub-sampled image, a reference point (P1) given by the centroid of the layer containing the maximum blood pool occupied by the MGB. For this point, the manual coordinates that unambiguously establish their spatial location in each considered image are identified.

iii) An LSSVM is implemented to recognize and detect point

P1. For this, the processes of:

a) **Training**. Training circle circular neighborhoods of 10 pixels, manually traced by a neurosurgeon, containing both point P1 (markers) and regions not containing P1 (no markers) are selected as a training set. For the markers, the center of their respective neighborhoods coincides with the manual coordinates of P1, previously established.

Such neighborhoods are constructed on the axial view of a sub-sampled image of 64x64 pixels. The main reason why a single image is chosen, for each reference point, is because it is desired to generate a LSSVM with a high degree of selectivity, which detects only those pixels that have a high degree of correlation with the training pattern.

Then, each neighborhood is vectorized and, considering its gray levels, the attributes are calculated: mean, variance, standard deviation and median. Thus, both markers and non-markers are described by vectors (**Va**) of statistical attributes, given by: **Va** = [mean, variance, standard deviation and median].

Additionally, the LSSVM is trained considering the vectors **Va** as a training pattern and intoning the values of the parameters that control its performance, γ and σ^2. This approach, based on attributes, allows the LSSVM to do its work with greater efficiency, than when using the larger vector-based approach, which only considers the gray level of the elements of an image. The training set is constructed with a ratio of 1:10, which means that 10 non-markers are included for each marker. The tag +1 is assigned to the class made up of the markers; while the -1 tag is assigned to the class of non-markers, that is, the training work is done based on a binary LSSVM.

During training, a classifier with a decision boundary is generated to detect LSSVM entry patterns as markers or non-

markers. Subsequently, due to the presence of false positives and negatives, a process is applied that allows incorporating into the training set the patterns that the LSSVM initially classifies inappropriately.

In this sense, it was considered a toolbox called LS-SVMLAB and the Matlab15 application to implement an LSSVM classifier based on a radial base Gaussian kernel with parameters σ^2 and γ.

b) Detection. The trained LSSVMs are used to detect *P1*, in images not used during training. To do this, a trained LSSVM looks for this reference point, in the axial view, from the first to the last image that makes up each of the 7 databases considered.

The validation process carried out with LSSVM allows to identify, automatically, the coordinates for P1 which are multiplied by a factor of 8 units, in order to be able to locate them, in the images of original size. In this way, the aforementioned coordinates are used to establish the exact location of the seed voxel required by the GR for its initialization. Finally, as a synthesis, figure 4 illustrates the process followed to locate the seed voxel in the databases considered.

Figure 4. Synthetic diagram that illustrates the operability of the LSSVM for the detection of the seed voxel coordinates.
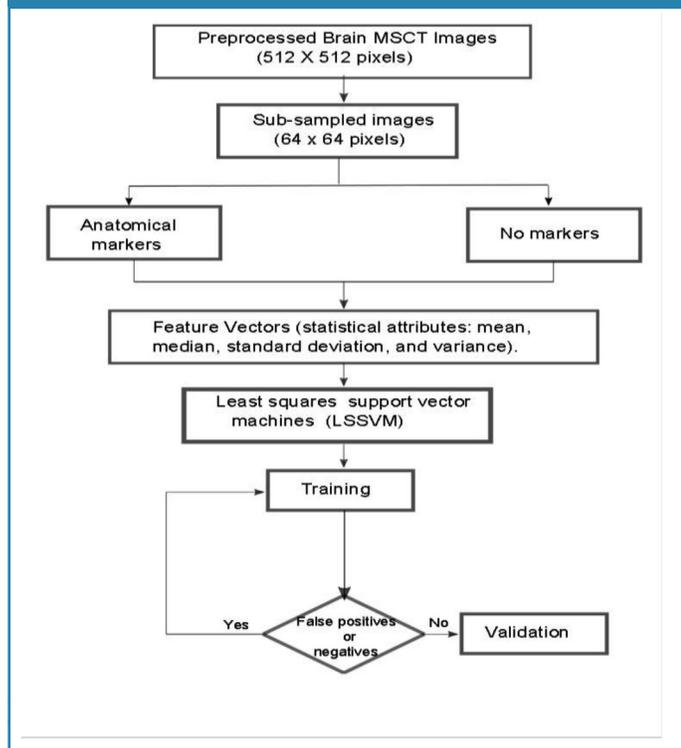
● Region growing (RG).

The region growing is an unsupervised clustering technique, which performs an iterative process that attempts to characterize each of the classes, according to the similarity between the voxels that integrate each of them and thus perform the segmentation[13]. The RG method allows grouping of the pixels or voxels belonging to the objects that make up an image ac-

cording to a predefined criterion. The RG requires a "seed" point which can be selected, manually or automatically, to extract all the pixels connected to seed[13].

To apply the RG, to the pre-processed images, the following considerations were made: a) The initial neighborhood, which is constructed from the seed, is assigned a cubic shape whose side depends on an arbitrary scalar *r*. The *r* parameter requires a tuning process. b) As a pre-defined criterion, modeling is chosen through Equation 5.

$$|I(x) - \mu| < m\sigma \qquad (5)$$

Where: I(x) is the intensity of the seed voxel, μ and σ the arithmetic mean and the standard deviation of the gray levels of the initial neighborhood and *m* a parameter that requires intonation.

● Parameters Tuning: Obtaining optimal parameters

The adequate performance of the proposed technique requires obtaining optimal parameters for each of the algorithms that comprise it. To do this, using DB1 as a reference, modify the parameters associated with the technique you wish to intone by systematically going through the values belonging to certain ranges, as described below.

o Dilation, erosion and Gaussian filters have the size of the observation window as a parameter. In order to reduce the number of possible combinations, an isotropic approach was considered to establish the range of values, which control the size of the window, which is given by the odd combinations, given by the following ordered lists: (1,1,1), (3,3,3), (5,5,5), (7,7,7) and (9,9,9).

o The parameters of the LSSVM, σ^2 and γ, are toned assuming that the cost function is convex and developing tests based on the following steps:

Ø To intone the parameter γ the value of σ^2 is arbitrarily set and values are systematically assigned to the parameter γ. The value of σ^2 is initially set at 2.5. Then, γ is varied considering the range [0,100] and a step size of 0.25.

● An analogous process is applied to intone the parameter σ^2, that is, γ is assigned the optimal value obtained in the previous step and, a step size of 0.25 is considered to assign to σ the range of values contained in the interval [0.50].

● The optimal parameters of the LSSVM are those values of γ and σ^2 that correspond to the relative minimum percentage error, calculated considering the manual coordinates of the reference seed, established by the neurosurgeon and the automatic ones generated by the LSSVM.

o During the intonation of the parameters of the RG, each of the automatic segmentations of the MGB corresponding to the DB1 described, is compared with the manual segmentations of the MGB generated by a neurosurgeon, considering the Dc. The optimal values for the parameters of the RG (*r* and *m*), are matched to that experiment that generates the highest value for the Dc.

The Dc is a metric that allows to compare segmentations of the same 2D or 3D image, obtained by different methodologies. In the medical context, usually, the Dc is considered to establish how similar are, spatially, manual segmentation (RD) and automatic segmentation (RP) that generates the morphology of any anatomical structure. Additionally, the Dc is maximum when a perfect overlap between RD and RP is reached but it is minimal when RD and RP do not overlap at all. In addition, the values expected for the Dc are real numbers between 0 (minimum) and 1 (maximum). The mathematical model de fining the Dc is given by Equation 6.

$$Dc = \frac{2|RD \cap RP|}{|RD| + |RP|} \qquad (6)$$

Results

Quantitative results

The optimal sizes for the expansion, erosion and Gaussian filters were (5,5,5), (3,3,3) and (3,3,3), respectively. Regarding the trained LSSVM, values of 2.00 and 1.25 were obtained as optimal parameters for γ and σ^2, respectively. The way to obtain these parameters is by means of the error that is presented when comparing the manual and automatic coordinates considering the percentage relative error (PrE). These values are associated with a minimum PrE of 3.78%.

The maximum value of the Dc obtained for the segmentation of the MGB is comparable with that reported in references[9,10,11], as is shown in table 2. For that maximum value the Rg generated optimal values of r and m are 10 and 7.0, respectively.

Table 2. Comparison of the average Dc generated both by the NLCT and by other techniques, reported in the literature, for the 3D segmentation of the EDH

Authors	Technique		Modality	Average
				Dc
Casamitjana et al.	Emerging	Neural	MRI	0. 9174
(2010)[9]	Networks			
Zhang et al.	FCNN		MRI	0.9050
(2017)[10]				
Kleesiek et al	Ilastik		MRI	0.7900
(2014)[11]				
Vera et al.	SCT		MSCT	0.8845
(Technique proposed in				
the present article)				

Qualitative results

Figure 5, shows a 2-D view of both the original MGB and the processed versions after applying the SCT.

Figure 5. Axial view of images belonging to DB1: a) Original, b) Dilated, c) Thresholdized, d) Erode, e) Smoothed with Gauss, f) Segmented with region growing technique.
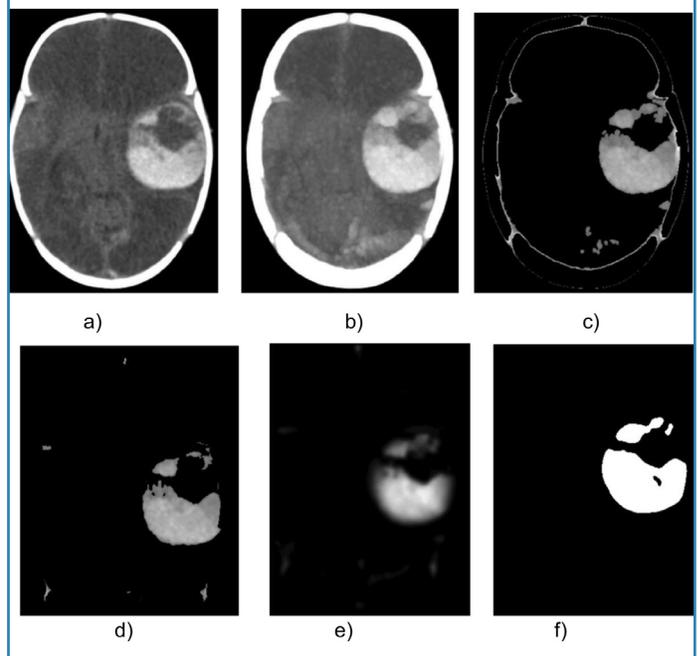
Conclusions

An accurate segmentation of brain tumors of the glioblastoma multiforme type, present in computed tomography images is achieved through the tuning process of an intelligent computational technique. This statement is based on the fact that the Dc obtained is comparable with that reported in the literature.

The use of intelligent operators, represented by the least squares vector support machines, allowed the automatic identification of the coordinates corresponding to the seed voxel which plays a crucial role in the adequate initialization of the unsupervised grouping algorithm based on region growing. In the immediate future, it is planned to use the segmentation generated by this technique to quantify the volume of the MGB. This volume is vital when deciding whether a patient is surgically treated or not to address the tumor that affects their health status.

References

1. Stelzer K. Epidemiology and prognosis of brain metastases. Surg Neurol Int. 2013;4(Suppl 4):S192-202.

2. Mcneill KA. Epidemiology of Brain Tumors. Neurol Clin. 2016;34(4):981-998.

3. American Brain Tumor Association (ABTA). About Brain Tumors: A Primer for Patients and Caregivers. 9ª Edition. 2015 ABTA.

4.   WHO (2007). Cavenee W, Louis D, Ohgaki H et al. Eds. WHO Classification of Tumours of the Central Nervous System. WHO Regional Office Europe.

5.   Ostrom Q., Gittleman H., Xi J., Kromer C., Wolinsky Y., Krinchko C., Barnholtz J., CBTRUS Statistical Report: Primary Brain and Central Nervous System Tumors Diagnosed in the United States in 2009-2013, Neuro Oncol (2016) 18 (suppl 5) v1-v75.

6. Vera M. Segmentación de estructuras cardiacas en imágenes de tomografía computarizada multi-corte. Ph.D. dissertation, Universidad de los Andes, Mérida-Venezuela, 2014.

7.   Maiera A, Wigstrm L, Hofmann H, Hornegger J, Zhu L, Strobel N, Fahrig R. Three-dimensional anisotropic adaptive filtering of projection data for noise reduction in cone beam CT. Medical Physics. 2011;38(11):5896–909.

8.   Kroft L, De Roos A, Geleijns J. Artifacts in ECG– synchronized MDCT coronary angiography. American Journal of Roentgenology.2007;189(3):581–91.

9.   Casamitjana A., Puch S., Aduriz A., Vilaplana V. (2017). 3D Convolutional Neural Networks for Brain Tumor Segmentation: a comparison of multi-resolution architectures. arXiv:1705.08236v1.

10. Zhang, J., Shen, X., Zhuo, T., & Zhou, H. (2017). Brain Tumor Segmentation Based on Refined Fully Convolutional Neural Networks with A Hierarchical Dice Loss. arXiv preprint arXiv:1712.09093

11. Kleesiek, J., Biller, A., Urban, G., Kothe, U., Bendszus, M., & Hamprecht, F. (2014). Ilastik for multi-modal brain tumor segmentation. Proceedings MICCAI BraTS (Brain Tumor Segmentation Challenge), 12-17.

12. Serra J. Image Analysis Using Mathematical Morphology. London, England: Academic Press, 1982.

13. W. Pratt, Digital Image Processing. USA: John Wiley & Sons Inc, 2007.

14. Mukhopadhyay S., Chanda B. A multiscale morphological approach to local contrast enhancement. Signal Processing, vol. 80, no. 4, pp. 685–696, 2000.

15. Yu Z., Wei G., Zhen C., Jing T., Ling L. Medical images edge detection based on mathematical morphology. En Proceedings of the IEEE Engineering in Medicine and Biology 27th Annual Conference, Shanghai–China, September 2005, pp. 6492–6495.

16. Sezgin M., Sankur B. Survey over image thresholding techniques and quantitative performance evaluation. Journal of Electronic Imaging, vol. 13, pp. 146–165, 2004.

17. Meijering H. Image en enhancement in digital X ray angiography. Tesis de Doctorado, Utrecht University, Netherlands, 2000.

18. V. Vapnik, Statistical Learning Theory. New York: John Wiley & Sons, 1998.

19. E. Osuna, R. Freund, y F. Girosi, "Training support vector machines: an application to face detection." en Conference on Computer Vision and Pattern Recognition (CVPR '97), San Juan, Puerto Rico, 1997, pp. 130–136.

20. A. Smola, "Learning with kernels," Tesis de Doctorado,Technische Universitt Berlin, Germany, 1998.

21. B. Scholkopf y A. Smola, Learning with Kernels: Support Vector Machines, Regularization, Optimization, and Beyond. Cambridge, MA , USA: The MIT Press, 2002.

22. J. Suykens, T. V. Gestel, y J. D. Brabanter, Least Squares Support Vector Machines.UK: World Scientific Publishing Co., 2002.

23. M. Oren, C. Papageorgiou, P. Sinha, E. Osuna, y T. Poggio, "Pedestrian detection using wavelet templates," en CVPR '97: Conference on Computer Vision and Pattern Recognition (CVPR '97). Washington, DC, USA: IEEE Computer Society, 1997, pp. 193–200.